Mem. S.A.It. Suppl. Vol. 26, 85

Memorie della
Supplementi

Continuing developments in the search for the Martian atmospheric methane

F. Mancarella[1], G. Liuzzi[2], S. Fonti[1], T.L. Roush[3], M.R. Chizek[4], J.R. Murphy[4], and A. Blanco[1]

[1] Università del Salento, Dipartimento di Matematica e Fisica 'Ennio De Giorgi', Via per Arnesano, 73100 Lecce, Italy, e-mail: francesca.mancarella@le.infn.it
[2] Università degli Studi della Basilicata, Scuola di Ingegneria, Via dell'Ateneo Lucano, 10, 85100 Potenza, Italy
[3] NASA Ames Research Centre, Planetary Systems Branch, Moffett Field, CA, USA
[4] New Mexico State University, Department of Astronomy, Las Cruces, NM, USA

Abstract. This work illustrates our latest developments in the issue of retrieving the amount of methane in the Martian atmosphere using the Thermal Emission Spectrometer (TES) data. Starting from the work of Fonti & Marzo (2010), we have carried out an analysis on the temporal trend of the methane content comparing it with the temporal trend of other species present in the Martian atmosphere. We have also developed and applied a pre-processing procedure to the TES spectra in order to retain the best data for the final detection of the methane band and the evaluation of its abundance. The spectra have been analyzed with the same statistical clustering as Fonti & Marzo (2010) but using the band depth instead of the two adjacent emissivity values.

Key words. Mars – Methane – Thermal Emission Spectrometer – Clustering technique

1. Introduction

In recent years, the presence of methane in the Martian atmosphere has been proposed by several authors (Krasnopolsky et al. 2004; Formisano et al. 2004; Mumma et al. 2009). Several mechanisms able to produce methane have been discussed in the literature including cometary infall (Formisano et al. 2004), $H_2O - CO$ photolysis (Bar-Nun & Dimitrov 2007), serpentinization (Oze & Sharma 2005) and biological origin (Formisano et al. 2004; Krasnopolsky et al. 2004). An important point stressed by Geminale et al. (2008) was that the methane mixing ratio in the Martian atmosphere is not constant, showing a spatial and temporal variability.

In this context the work of Fonti & Marzo (2010) is particularly important. Using a statistical clustering technique, they analyzed $\approx 3 \times 10^6$ Thermal Emission Spectrometer (TES) spectra, spanning three Martian Years. At the principal L_s values investigated (i.e. 0°-90°-180°-270°), the methane content has an annual cycle and a recurrent spatial distribution with higher values over Tharsis, Arabia Terrae and Elysium as shown in Fig. 1 (Fonti & Marzo 2010).

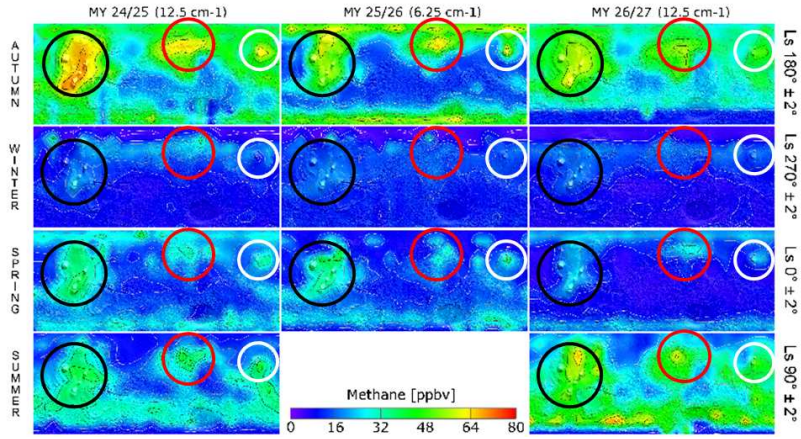

Fig. 1. Methane spatial distribution from Fonti & Marzo (2010) superimposed on a Mola map at eleven different times in L_s for three MYs. The black circle indicates the location of the Tharsis region, the red Arabia Terrae and the white Elysium.

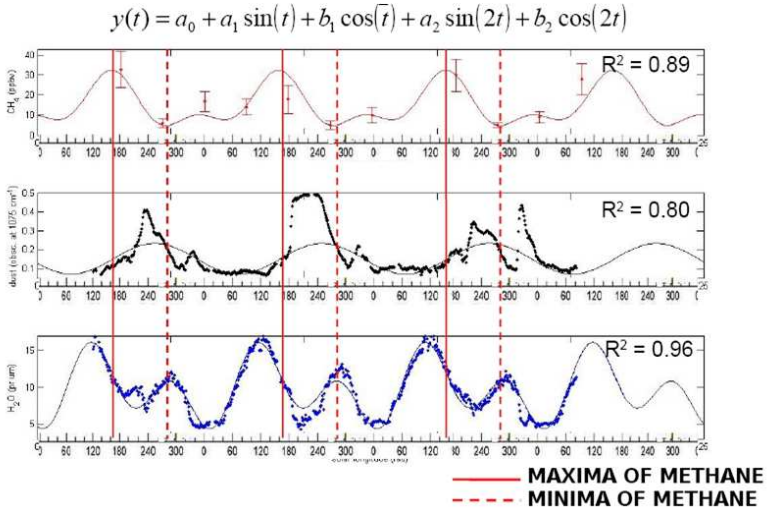

Fig. 2. Seasonal variation of the global methane content in Martian atmosphere (top panel) compared to the data analyzed by Smith (2004) for atmospheric dust (central panel) and water vapor (bottom panel). The data, interpolated with a double sinusoidal function, seem to suggest a possible methane cycle, with precise phase correlations to dust and water vapor cycles. The two red vertical lines mark the maxima (solid) and minima (dashed) of the interpolated methane.

In this work we illustrate our last analysis of the TES data in order to validate and improve the results obtained by Fonti & Marzo (2010).

2. Methane seasonal cycle

In order to understand if the results of Fonti & Marzo (2010) follow a regular cycle the global

methane content has been evaluated as a function of the time and the trend has been fitted with the composite sinusoidal function:

$$y(t) = a_0 + a_1 sin(t) + b_1 cos(t) + \\ + a_2 sin(2t) + b_2 cos(2t)$$

where the values of the five parameters a_0, a_1, a_2, b_1 and b_2 have been adjusted using the χ^2 technique in order to obtain the best fit. The result is reported in the top panel of Fig. 2. A similar analysis was performed for the aerosol opacity and water vapor cycle (Smith 2004). The data and fits are shown in the middle and bottom panels, respectively, of Fig. 2. The main methane maximum does not coincide with the dust maximum and occurs after the main water vapor maximum. The main methane minimum is located just after the dust maximum and coincides with the secondary maximum of water vapor.

Clearly, a better understanding of any relationships between the methane present in the Martian atmosphere and the dust aerosol and the water vapor abundance would benefit from higher temporal sampling of the global methane content.

3. Cleaning the TES data

In order to increase the temporal sampling of the methane annual cycle, and to improve our confidence in the results obtained by Fonti & Marzo (2010) we focused on removing anomalous spectra (e.g. Fig. 3) from the TES data. The presence of such spectra could affect the statistical analysis by increasing the uncertainty in the final derived methane content.

We have developed a cleaning process that is applied before the statistical clustering is performed. In the following sections we show some results of this pre-processing procedure applied to the data of $L_s = 180° \pm 5°$ of MY24, 977561 spectra.

3.1. Lower and upper limit

The first and last 10 channels of the TES spectra exhibit a significant variability and as results, are excluded from our analyses. We first removed all spectra which have an emissivity value, in any spectral channel, outside the range 0.05-1.10. The lower limit was defined after we confirmed that the bottom of the CO_2 main band at 670 cm^{-1}, was not affected.

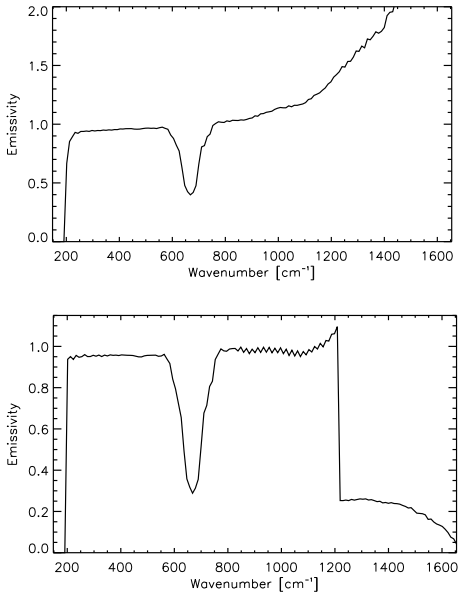

Fig. 3. Two examples of anomalous spectra, belonging to the dataset $L_s = 180° \pm 5°$ MY24. In the top panel a spectrum with emissivity values increasing constantly well above 1 in the high wavenumber region. In the bottom panel a spectrum showing a sudden drop in emissivity at about 1200 cm^{-1}.

The calibration procedure of the TES radiance data affects the spectral region around the methane band and the resulting emissivity spectra may have a level ≥ 1. The upper limit was defined after confirming that only anomalous spectra were removed from the dataset. The number of spectra remaining after this preliminary step was 843620.

3.2. Ripple removing

As shown in the bottom panel of Fig. 3 and enhanced in Fig. 4 in the 800 – 1100 cm^{-1} range, some spectra present a regular peak-to-peak variability, hereafter *ripple*. This could be very dangerous for our analysis because the methane band has exactly the same behavior as a single period of a *ripple*.

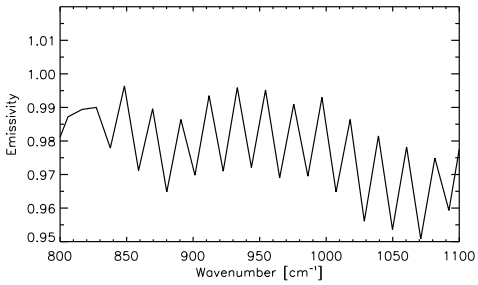

Fig. 4. Zoom of the bottom panel of Fig. 3 in the range 800 – 1100 cm^{-1} showing a *ripple* with a two channels periodicity.

To address this issue we have defined a Ripple Parameter (RP), given by:

$$RP = \frac{\Sigma_{even}\epsilon}{\Sigma_{odd}\epsilon} \quad (1)$$

where $\Sigma_{even}\epsilon$ and $\Sigma_{odd}\epsilon$ are the sum of all the emissivity values in the even and odd channels, respectively, of the spectral range 1200 – 1400 cm^{-1}. If the peak-to-peak variability is small and the emissivity values are randomly distributed, then the value of the RP would tend to one. If a *ripple* with a large enough amplitude is present, then the RP value will be higher or lower than one by an amount depending on the *ripple* amplitude. All TES spectra where $0.99 < RP < 1.01$ are retained for further analysis. The number of spectra removed by this process was 72860.

3.3. Pre-processing results

The application of both steps of the pre-processing procedure to the TES data has removed a total of only 206801 spectra leaving $\approx 79\%$ of the total data for further analyses.

The benefit of the pre-processing procedure is illustrated in Fig. 5 where the average of the spectra before (top panel) and after (bottom panel) pre-processing are shown along with their associated standard deviations. Both spectra are very similar at low wavenumbers, but differences are significant at higher wavenumbers (from 1200 cm^{-1} to 1600 cm^{-1}), where the methane band is located. Significant differences are also evident in the decrease of the standard deviations near the main CO_2 band (670 cm^{-1}) and the dust band (1100 cm^{-1}).

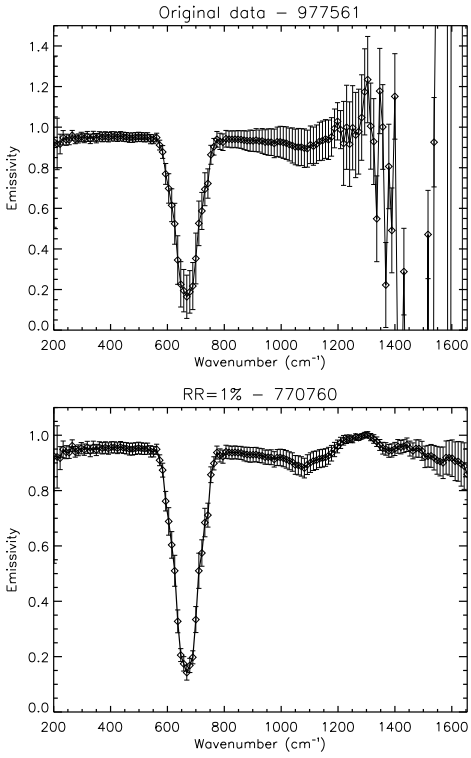

Fig. 5. Top panel: Average of the 977561 TES spectra belonging to $L_s = 180° \pm 5°$ of the $MY24$ without any pre-processing. Bottom panel: Average of the remaining 770760 TES spectra after applying the lower and upper limit and setting the RP at 1%.

4. Clustering the TES data

As shown in the previous section the pre-processing procedure allows to retained the spectra most promising for the detection of Martian methane and the evaluation of its content.

In Fonti & Marzo (2010) the selection criterion used for statistical clustering was based on the emissivity values in the methane channel (1304 cm^{-1}) and the adjacent channel at lower wavenumbers (1294 cm^{-1}). After some tests, we found that this criterion could produce

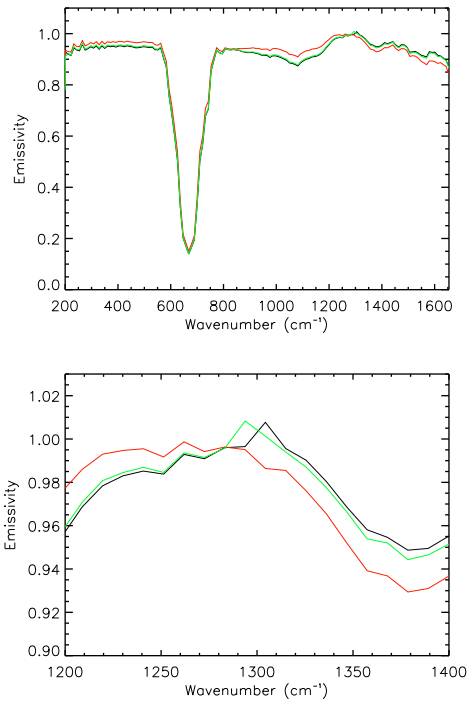

Fig. 6. Top panel: Example of the application of clustering procedure using the criterion of Fonti & Marzo (2010): the three spectra represent the average of the spectra contained in each cluster. Bottom panel: The same spectra as in the top panel but in the spectral range 1200 – 1400 cm^{-1}.

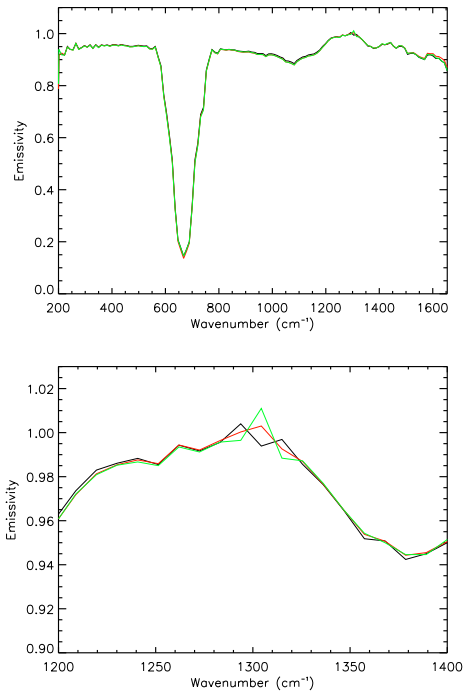

Fig. 7. Top panel: Example of the application of clustering procedure using the BD as clustering criterion: the three spectra represent the average of the spectra contained in each group created by the clustering. Bottom panel: The same spectra as in the top panel but in the spectral range 1200 – 1400 cm^{-1}.

some unwanted effects as shown in Fig. 6. The red spectrum has an absorption band similar to methane but the overall behavior is different from the other two. The point of the distortion of the spectra is coincident with the channel were the TES radiance spectra are normalized to obtain the corresponding emissivity spectra. Therefore, in the example shown in Fig. 6, the clustering procedure may have grouped the spectra according to the albedo values and/or the surface temperature.

In order to address this issue, we decided to adopt a new selection criterion based on the value of the methane Band Depth (BD), defined as (Clark & Rush 1984):

$$BD = 1 - \frac{b}{c} \quad (2)$$

where b is the emissivity value in the channel corresponding to the methane band and c is the average emissivity value of the nearby continuum, i.e. the average of the two emissivity values on each side of the band. Fig. 7 reports the results of the clustering procedure, applied to the same data set of Fig. 6, but using the BD. The spectra of the three clusters have the same overall behavior for the entire spectral range and differ chiefly in the region of the methane band.

As test, we investigated more carefully the spectra contained in the group represented by the central spectrum of Fig. 7 (red curve). In fact, applying the clustering procedure to this cluster we obtain two clusters, as shown in Fig. 8. To emphasize the presence of the methane signature in the black spectrum of the top panel

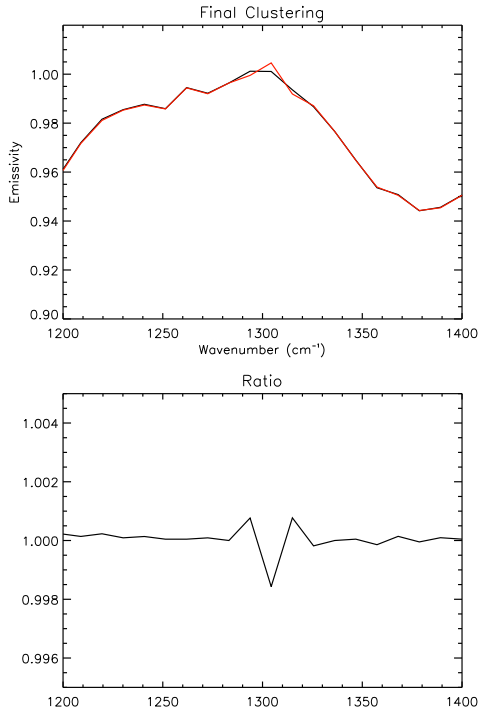

Fig. 8. Top panel: Averages of the spectra after the final application of the clustering procedure. Bottom panel: Ratio between the total average of the analyzed spectra and the spectrum not containing the methane signature (the red spectrum in the top panel).

of Fig. 8, we show in the bottom panel the ratio between the average of all the spectra contained in the red and black group and the red spectrum in the top panel of Fig. 8.

5. Conclusions

In this work we have described the efforts made in searching the methane signature in the Martian atmosphere, using the TES spectra and a statistical clustering procedure.

The pre-processing procedure developed here removes effectively unwanted spectra having very high and very low emissivity values. It helps to remove also the spectra with a regular peak-to-peak variability behavior, called *ripple*, that could affect the detection of the methane band (as shown in Fig. 5).

We have also tested if the clustering criterion used in Fonti & Marzo (2010) could be improved. The comparison of the Fig. 6 and 7 clearly shows that the introduction of the band depth (BD) criterion improves the capacity of detecting the methane band without introducing spurious effects.

In future, we will focus on improving the pre-processing procedure to remove any systematic and random behavior(s) that affect the data and that could be interpreted as methane signature in the spectra. The production of a data set of synthetic spectra will help to better understand how all the atmospheric components of the Martian atmosphere, and in particular the methane, influence the spectral behavior of TES data. The synthetic spectra will also contribute for a more accurate retrievals of the methane abundance contained in the atmosphere.

References

Bar-Nun, A., & Dimitrov, V. 2007, Icarus, 188, 543
Clark, R.N., & Roush, T.L. 1984, J. Geophys. Res., 89, 6329
Fonti, S., & Marzo, G. 2010, A&A,512
Formisano, V., et al. 2004, Science, 306, 1758
Geminale, A., Formisano, V., & Giuranna, M. 2008, Science, 56, 1194
Krasnopolsky, V.A., Maillard, J.P., & Owen, T. C. 2004, Icarus, 172, 537
Mumma, M.J., et al. 2009, Science, 323, 1041
Oze, C., & Sharma, M. 2005, Geophys. Res. Lett., 32
Smith, M.D. 2004, Icarus, 167, 148